4. MODULATED ELLIPTICAL SLOT

Cost effective near- and far-field high-resolution microwave and millimeter wave imaging systems can be implemented using array of modulated elements [14]. As discussed in the previous section, modulating the array elements in time, facilitates spatial tagging of the incident electromagnetic field on the array spatial region, and hence, a 2D map of that field can be obtained using a single receiver (which simplifies the design considerably) [14]. Basically, modulation allows the array element to "tag" its own signal, and that not only provides a mean for the receiver to identify the location from which the signal was received, i.e., spatial multiplexing, but also enhances signal detection. This is true since from the detection point of view modulated signals are distinct from the non-coherent clutter in the environment and receiver noise. The higher the modulation depth is, i.e., how well the array elements can modulate the incident electric field, the higher is the sensitivity of the imaging system to small variations in the measured field.

As pointed out earlier, since the conventional MST uses small loaded dipoles, which result in compact array for better field sampling, they suffer from major drawbacks. The inefficiency of small dipoles limits the modulation depth and the SNR (less than 2% modulation depth was observed in Section 3). Since the modulated scattered signal level from an MST array dipole is typically very small, the robustness of the conventional MST system is undermined by the residual carrier problem (carrier suppression through tuning is needed each time the measurement setup changes). Furthermore, the mutual coupling among the array dipoles can significantly limit the system dynamic range. At high frequency, these problems render the implementation of such MST imaging array very challenging, i.e., the SNR/sensitivity factor derived in the previous section becomes very small.

From the previous analysis, it was concluded that, in order to improve upon the conventional MST, an efficient array element should be used instead of the short dipole. To this end, a modulated slot may be utilized in the imaging array. The selection of the slot is justified by the fact that microwave and millimeter wave signals can pass though a slot with minimum attenuation if the slot is properly designed. In its simplest form, once MST is applied to slots, it implies that the required modulation

is achieved by opening and closing the slot (allowing the signal to pass or not pass through the slot, respectively). Modulation depth close to 100% can be achieved when the slot is modulated between open- and close-states. Therefore, with modulated slots, the imaging system sensitivity can be considerably enhanced compared to the MST arrays based on dipoles.

To illustrate the basic idea behind using modulated slots in imaging systems, consider Figure 4.1 which shows a generic implementation of such system based on array of modulated slots [18]. The slots shown in Figure 4.1 are cut into a conducting screen (non-transparent to EM fields) and the receiver is placed behind that screen. The electric field distribution of interest is measured by opening and closing the slots via controlling their loads. At the initial state, all slots are closed and no signal passes through to the receiver. When any given slot is opened, while the rest are closed, the respective electric field at the particular location of the open slot only is coupled into that slot and subsequently, re-radiated into the opposite side of the screen where it is picked up by the receiver. Each slot is modulated, by opening and closing it, at a certain modulation rate. In this way, the electric field due to each slot can be individually discriminated and measured using a single receiver.

In imaging applications, the effect of the reflection from the array due to the conducting screen should be accounted for properly, i.e., through calibration. When all slots are open, the array becomes transparent to the EM waves at the frequencies where the slots are efficient (spatial band-pass filter) [55]. When most of the slots are closed, the reflected waves from the array might interact with the source of the incident field, i.e., the object to be imaged. Multiple reflections between the array and the source may change the field distribution of interest. This situation can be resolved in practice by increasing the distance between the array and the source. Measuring the field of interest at multiple array-source distances can reduce the effect of multiple reflections considerably. Using absorbing material to cover the exposed conductor on the array can also reduce these reflections to a large extent. Similar remedies are typically used with the conventional MST arrays of dipoles and can be applied to the array of slots [51].

In order for the imaging scheme described above to work, the slot should be designed such that it can be opened and closed completely and respond very quickly

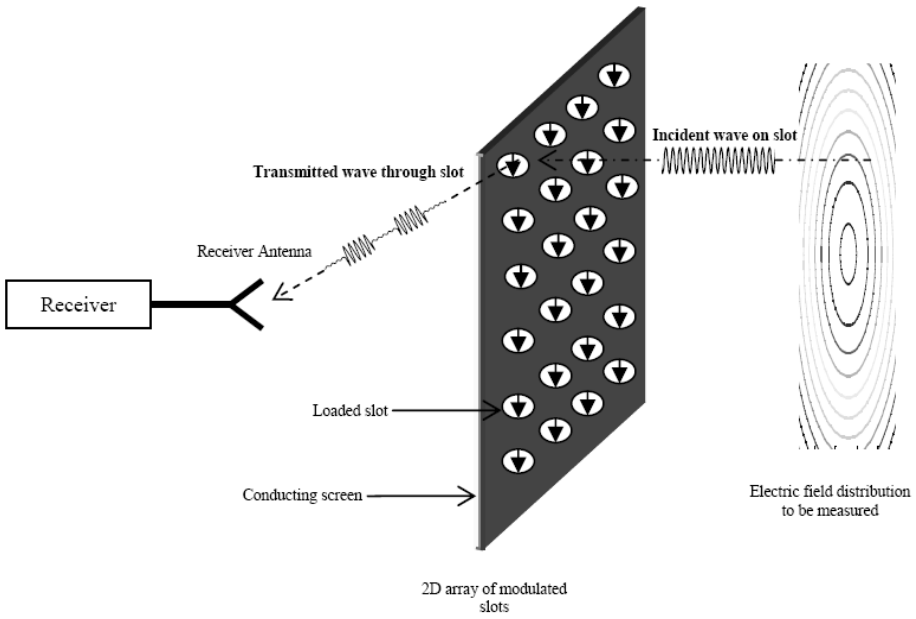

Figure 4.1. Generic implementation of an imaging system based on array of modulated slots.

to an electronic control signal. The dimensions of the slot (in both directions) should be less than $\lambda/2$ for proper electric field sampling (to prevent aliasing as dictated by the Sampling Theorem [54]). A design of a slot which meets these requirements will be presented next.

4.1. MODULATED SLOT DESIGN

Since they are relatively easy to manufacture and possess a low profile as flush-mounted antennas, slots in conducting ground planes are used extensively in many applications [56]. Recently printed elliptical and circular slot designs have received considerable attention for realizing ultra-wideband antennas for wireless communication systems (comprehensive reviews of the most recent designs can be found in [57] and [58]). Here, the design of a novel, compact and resonant slot for imaging system realizations is presented. The advantages of using resonant slots are multifold. First, the resonant slot can have, through special loading, a small form-factor. Second, with

small resonant slots, the mutual coupling between various array slots can be significantly reduced (see [59] and the references therein). Furthermore, once the resonant slot is used as a modulated element, the modulation depth can be maximized toward enhancing the sensitivity of the imaging system. These advantages working together not only make the imaging system highly sensitive, but also promote high-resolution imaging [18].

Figure 4.2(a) shows the schematic of the designed modulated resonant slot. The designed slot has an elliptical shape with major and minor radii r_1 and r_2, respectively, cut into a conducting plane. This slot is linearly polarized along the direction of the ellipse's minor axis, i.e., y-axis, and it has a broadside radiation pattern with wide beamwidth. For imaging purposes, it is advantageous to have a wide radiation beam pattern. Slots with wide-beam radiation pattern posses very low spatial selectivity and thus insure detection from all directions. Furthermore, for synthetic array processing, e.g., SAFT, wide-beam patterns are also desirable in order to attain the maximum possible spatial resolution.

In order to realize a compact array, the largest dimension of the slot must be less than half-wavelength. Hence, the elliptical slot by itself will be a sub-resonant inductive slot. To make the slot resonates at a certain frequency, it is loaded by a conductive circular load of radius r_L, as shown in Figure 4.2(a). In essence, the gap of length L_g, shown in Figure 4.2(a) between the circular load and the edge of the elliptical slot, adds capacitance to the overall slot structure. Consequently, the inductive elliptical slot and the capacitive gap element result in a single resonant structure. This is true even though the largest linear dimension in the overall slot structure is less than half-wavelength. Such concept is typically followed to design resonant waveguide irises [59].

The resonance frequency of the elliptical slot structure shown in Figure 4.2(a) is function of the slot dimensions; namely r_1, r_2, and L_g ($L_g = r_2 - r_L - s$). Thus, one can control/change the resonance frequency by changing these (interdependent) dimensions. Primarily, reducing r_1 and r_2 increases the resonance frequency. Increasing L_g makes the slot resonate at lower frequencies. The obtained bandwidth around the resonance freqeuncy is a function of the slot axial ratio r_2/r_1. On the other hand, since the resonance frequency is a function of the slot capacitance, this frequency

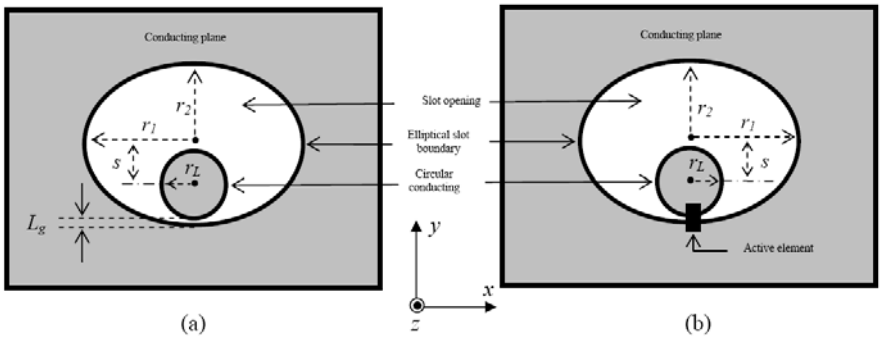

Figure 4.2. Schematic of the designed elliptical slot (a) with, and (b) without the active element load.

can be controlled electronically via loading the slot with an active element, e.g., PIN diode, varactor diode, etc., as shown in Figure 4.2(b). Changing the properties, e.g., capacitance, of the active element, causes the resonance frequency to change. In general, when the active element is capacitive, its capacitance is added to the gap capacitance, and consequently the resonance frequency decreases compared to the unloaded slot case shown in Figure 4.2(a). The properties of the active element can be controlled electronically, e.g., by a dc control voltage applied across the element. This effect is used to modulate the slot in time, i.e., opening and closing it.

Near or in the millimeter wave region, the capacitance of typical active elements available nowadays in the market might not change sufficiently in response to their control signal. Thus, such elements cannot be arbitrarily selected and placed to load the slot because they might not produce the desired change in the resonance frequency of the slot. Therefore, in order to attain an efficient control over the slot properties, the active element should be placed in high-intensity electric field region where it can cause maximum field perturbation. Consequently, the slot resonance frequency changes as desired in response to a change the in the electrical properties of the active element. In order to realize this concept, the electric field is "forced" to concentrate in one region between the elliptical slot boundary and the circular load. This is the main reason behind offsetting the circular load center from the elliptical slot center by certain amount, s, toward one of the boundaries (basically forming a small gap with high field density). This offset has the effect of "trapping" the electric

field in the region between the elliptical slot boundary and the circular load. Thus, the slot capacitance is primarily determined by the gap and whatever else placed near that gap, i.e., the active element. Consequently, the resonance frequency of the slot can be properly controlled with commercially available active loads.

It must be mentioned here that the desired capacitance change can be synthesized using combination of active elements and distributed loads, i.e., transmission line stubs. Such an option, however, is not always feasible for compact array designs since it requires additional space around the slot area. For compact array design used for high resolution imaging, the array spatial area is typically cramped by the slots themselves and the control bias lines routed to each slot.

Loading the slot with a PIN diode is of particular interest here since it allows the desired rapid control effect (switching time in order of few nanoseconds) and consumes relatively small amount of power. When the diode is forward-biased (turned ON), its resistive impedance “shorts” the gap between the circular load and the elliptical slot edge, and consequently, the slot (actually its dominant field mode) does not resonate in the band, i.e., at the frequency of interest where the receiver is expecting a signal. In this state, the slot does not allow any signal to pass through, i.e., the slot is "closed". When the diode is forward biased, it represents a capacitive load which adds to the gap capacitance and makes the slot resonate at the design frequency of interest, and hence, signals at that frequency pass through the slot, i.e., the slot is "open". Consequently, maximum modulation depth can be achieved. In practice however, the modulation depth may be reduced due to signal leakages (when the slot is closed) and losses (when the slot is open).

4.1.1. Field Distributions. Studying the electric field and the current distributions in and around the slot area, respectively, is vital for proper slot design as well as for understanding its behavior, i.e., mutual coupling, when it is placed near another slot in an array. For imaging applications where the objective is to measure the relative electric field in a certain spatial domain, it is important to make sure the slot is sensitive to the field component of interest (proper polarization) and that it provides a response proportional to the local incident field on it (obtaining localized field measurements).

Numerical electromagnetic simulations were performed to investigate various attributes of the designed PIN-diode loaded elliptical slot. To this end, CST Microwave Studio® commercial simulation package was used [60]. Although many idealistic simulation models were considered in the early stages of slot prototyping, i.e., using perfect electric conductors, PIN diode with zero-ohm forward resistance, etc., the results presented here are obtained from simulating a practical 24 GHz elliptical slot on a printed circuit made of a lossy conductor, i.e., copper. The PIN diode in the ON and OFF states was modeled as a lumped element with impedance of 5 Ohm and $-j265$ Ohm (at 24 GHz), respectively. In simulation, the slot was fed by a K-band rectangular waveguide aperture with finite flange of size 21 mm $\times$ 21 mm, i.e., the slot was mounted on the flange. Table 4.1 lists the dimensions of the simulated slot. The design specifics of this slot will be described later in this section.

Table 4.1. K-band resonant elliptical slot dimensions (Resonance frequency: 24 GHz).

Parameter	**Dimension (mm), [mils]**
r_1	2.36, [93]
r_2	1.78, [70]
r_L	0.78, [31]
s	0.58, [23]

Figures 4.3 and 4.4 show typical normalized spatial distributions of the electric and magnetic field components (in the x, y, and z directions) for the simulated resonant elliptical loaded slot at 24 GHz (the PIN diode is not shown in the figures). The field distributions for both the ON and OFF PIN diode states are provided in Figures 4.3 and 4.4. As shown in these figures, when the diode is in the OFF state (slot is open), the field components E_y and H_z are much higher than the rest of their respective components. This indicates that the slot fields are mainly linearly polarized. The slot is shown to be mostly sensitive to electric fields polarized along the y-axis. It is also shown that the fields are more concentrated around the circular load and the gap area between that load and edge of the elliptical slot when the slot is open. Consequently, the integral of the field over the slot area is largely determined by the

fields distributed in the small area around the circular load. This basically means that the slot is more sensitive to the local incident fields on that small area rendering localized field measurements as desired. It is also interesting to note that, the signal couples into the slot when it is open primarily via the magnetic field component H_z (slots in general provide higher magnetic coupling).

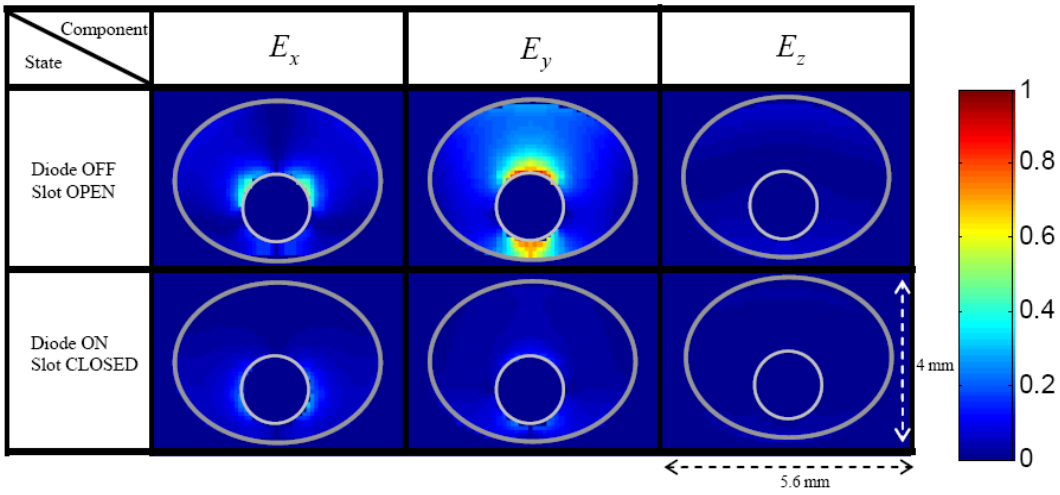

Figure 4.3. Distributions of the three electric field components in the slot area for both ON and OFF diode states.

When the PIN diode is turned ON, Figures 4.3 and 4.4 show that the electric and magnetic fields reduce significantly compared to the OFF PIN-diode state. This is especially true in the electric field case shown in Figure 4.3 where the magnitudes of the three field components become almost zero in the slot area when the diode is turned ON. Hence, in the ON PIN-diode state, the slot blocks the signal and does not allow it to pass through; that is, the slot is closed.

When the PIN diode is turned ON (slot is closed), the magnetic field component H_z remains relatively high around the area where the PIN diode is located as shown in 4.4. The coupled energy into the slot due to this component when the diode is turned ON (slot is closed) is not totally radiated by the slot. Large portion of this energy is dissipated in the forward-bias resistance of the PIN diode. However, the

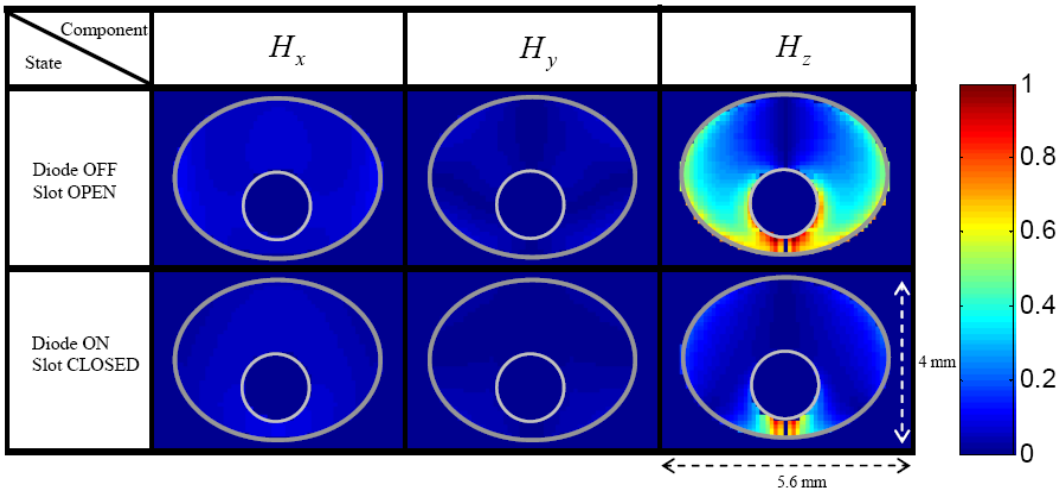

Figure 4.4. Distributions of the three magnetic field components in the slot area for both ON and OFF diode states.

remaining small portion actually gets radiated, i.e., it induces a current on the slot structure. Consequently, the slot can not be completely closed, and this in turn, may reduce the obtained modulation depth slightly compared to the ideal zero-ohm PIN diode case as it will be shown later.

Examining the surface current distribution on the slot structure gives valuable insight about its behavior when it is open and closed. The surface current distribution follows the distribution of the tangential components of the magnetic field. Figures 4.5(a)-(b) show the magnitude distribution of the tangential components (x and y) of the magnetic field around the slot area in the ON and OFF PIN diode states, respectively (note that Figures 4.5(a)-(b) have different scales/color-bars). When the slot is open, the 24 GHz signal induces a current density on the metallic structure around the slot as shown in Figure 4.5(a). In this case, the slot radiates efficiently. The high current density around the diode location indicates that most of the current actually passes through that point.

When the diode is turned ON (the slot is closed), small amount of energy is coupled into the slot and this energy hardly induces any radiating currents around the slot as shown in Figure 4.5(b). In this case, high current density is observed again around the diode. As pointed out before, in this state, the diode represents a

resistive load, and consequently, most of the energy coupled into the slot (due to H_z) is dissipated in the diode.

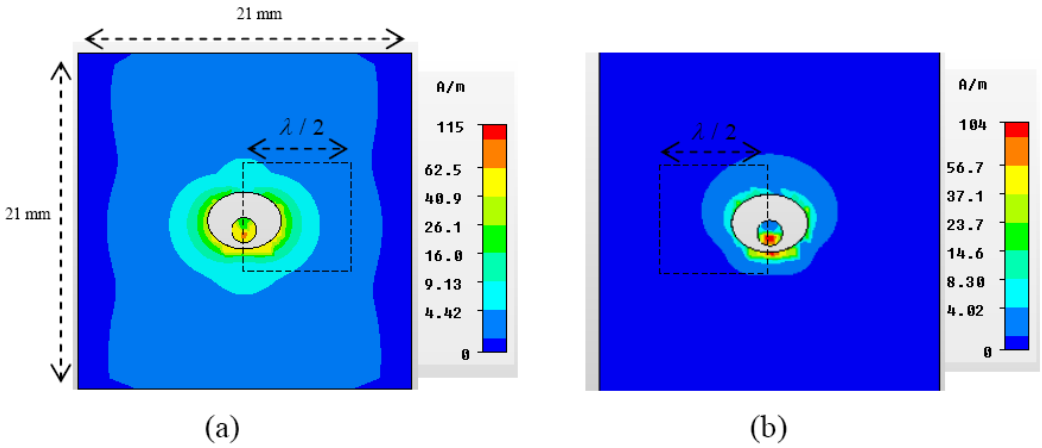

Figure 4.5. Tangential magnetic field distributions ($\propto$ surface current density) around the slot for (a) OFF and (b) ON diode states.

In 2D imaging arrays, the slots will be placed near one another within $\lambda/2$ side-by-side along the x-axis (H-plane) and in a collinear arrangement along the y-axis (E-Plane). Typically and as described before, one of the slots will be open while the rest in the array are closed at any given time. The interaction (transfer of energy) between the open slot and remaining closed slots constitutes the so called "mutual coupling". From results presented in Figure 4.5(a)-(b), it can be seen when two slots are placed in a collinear arrangement along the y-axis, they will interact more than when they are placed side-by-side along the x-axis (the surface current in the former case extends and reaches out further than the latter). Mutual coupling between similar resonant slots (similar current distributions) was studied thoroughly via numerical simulation as well as experiments in the past by Abou-Khousa and *et al* [59]. It was found that the mutual coupling between such slots is actually very small (less than -20 dB for a typical $\lambda/2$ interspacing).

4.1.2. Far-Field Radiation Pattern. Figures 4.6(a)-(b) shows typical far-field pattern of the designed loaded elliptical slot (diode OFF) presented in 3D

and rectangular plots, respectively. As shown in Figure 4.6(b), the 3-dB beamwidths in both principle planes (E- and H-planes) are around 50 and 60 degrees, respectively. Such wide beams in both planes are suitable for the imaging applications of interest as discussed before.

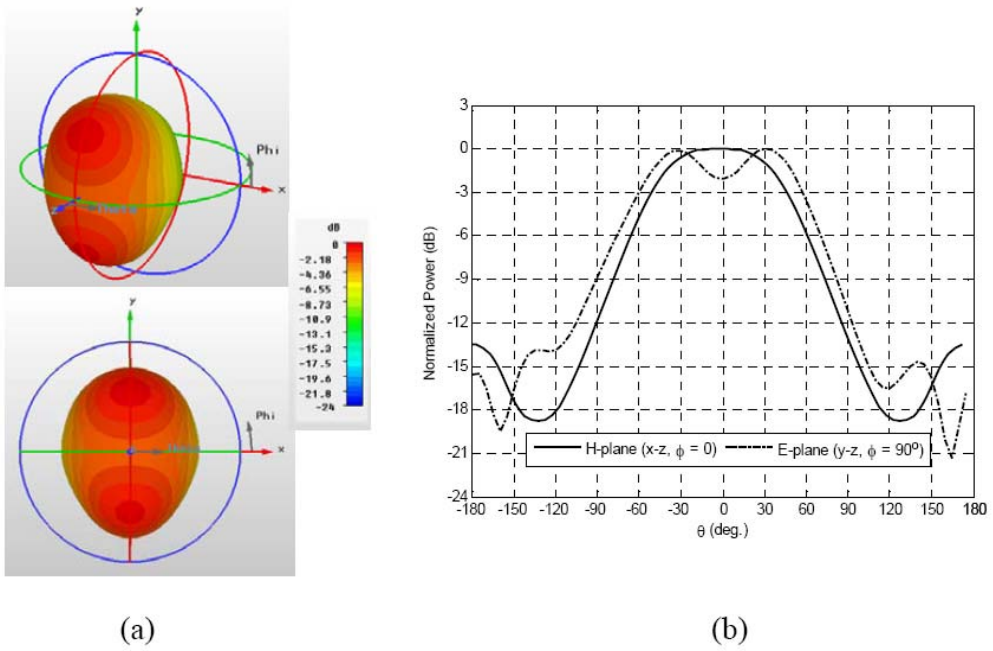

(a) (b)

Figure 4.6. Typical far-field pattern of the loaded elliptical slot (diode OFF) presented in: (a) 3D, and (b) rectangular plots.

The radiation efficiency of this slot is high as desired for sensitive field measurements (around 97%). Note that the ripple in the main beam of the E-plane pattern is mainly attributed to the finite ground plane effect [36], i.e., the flange size

was 21 × 21 mm (the surface current reaches the edge of the flange in that plane as shown in Figure 4.5(b)). This effect was confirmed via simulations.

4.2. K-BAND SLOT

To demonstrate the operation of the proposed resonant slot, an elliptical slot was designed to resonate at 24 GHz in the K-band (18-26.5 GHz) when loaded with a PIN diode.

4.2.1. Slot Design. Table 4.1 lists the pertinent dimensions of the designed slot. A magnified picture of the slot is given in Figure 4.7. The slot was manufactured using standard photolithographic printed circuit board (PCB) manufacturing technique on a Rogers4350 board of 0.020" (0.5 mm) thickness. Note that the free-space wavelength is around 12.5 mm (492 mils) at 24 GHz. The largest slot dimension, $2r_1 = 4.72$ mm, is a bit larger than one-third of the free-space wavelength. In fact, it is challenging to realize a resonant slot with these dimensions without special loading as in the case of this novel design.

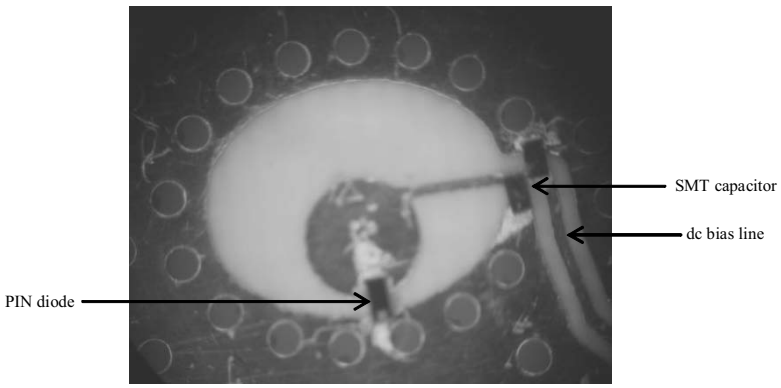

Figure 4.7. A magnified picture of the manufactured K-band slot and biasing structure.

Ma-com MA4GP907 flip-chip high frequency flip-chip PIN diode (0.63 mm × 0.38 mm) was used to load the slot [49]. The PIN diode was controlled by dc bias line (0.25 mm wide) routed to the circular load location, as shown in Figure 4.7.

In the slot opening region, the bias line was routed such that it was orthogonal to the dominant mode electric field polarization, and hence, its perturbing effect was minimized. The used PIN diode needed 1.45V to switch between the reverse the forward states. When reverse biased, the diode represents a capacitive load of ~ 25 (fF), and in the forward state it is equivalent to 5-Ohm resistive load. Additionally, 5-pF small surface-mount (SMT) capacitors (0.5 mm $\times$ 0.25 mm) were used to realize an RF return path to ground (short-circuit) for any signal that might couple into the dc bias lines, and thus preventing any spurious radiation or resonances that could result from such coupling.

4.2.2. Reflection Measurements. The slot was fed by a K-band rectangular waveguide and the input reflection coefficient, S_{11}, was measured using HP8510C Vector Network Analyzer (VNA), e.g., the waveguide was connected to port 1 of the VNA. Figure 4.8 shows a schematic of the measurement setup and the magnitude of the measured reflection coefficient, S_{11}, for the cases when no diode is used for loading, the diode is OFF and the diode is ON. Figure 4.8 also compares the experimental and numerical simulation results. From the measurement results, it is observed that when the slot is not loaded with the diode, it resonates at around 25.5 GHz (the point of minimum reflection).

Loading the slot with the reverse biased PIN diode (i.e. OFF) increases the overall capacitance and consequently shifts the resonant frequency to around 23.82 GHz as shown in Figure 4.8. This shift is expected since the diode is in parallel with the offset gap between the circular load and the edge of the elliptical slot. It is observed that the developed resonant slot has a 20 dB-return-loss bandwidth of 530 MHz centered around 23.8 GHz as indicated in Figure 4.8. At 24 GHz, when the diode is switched ON, the reflection is high indicating no signal is passing through the slot (reflection around -0.7 dB and the slot is closed). On the other hand, when the diode is switched OFF, the reflection coefficient at 24 GHz is very small indicating that most of the signal couples into the slot (around -22.8 dB and the slot is open). Thus, the modulation depth is maximized as it will be examined further later. It is also observed that the difference between the ON and OFF state over the 20 dB-return-loss bandwidth is larger than 19 dB. This will result in high modulation depth

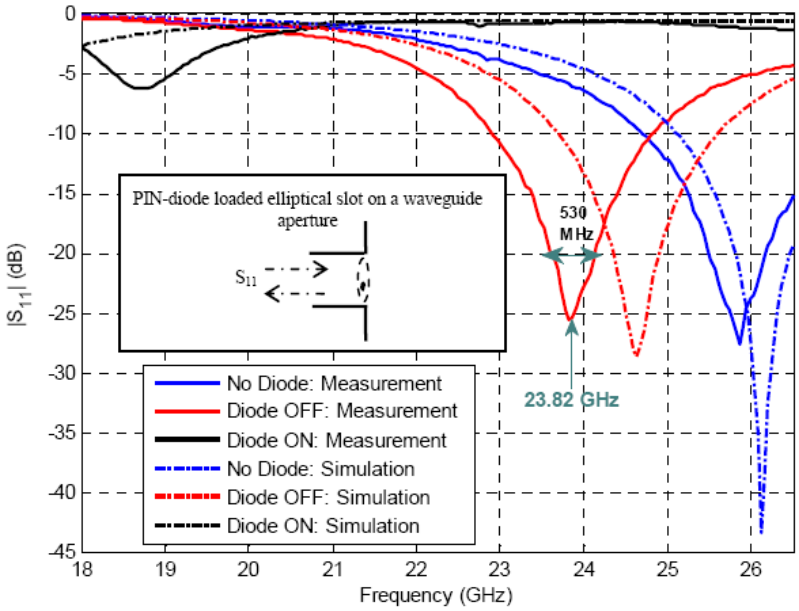

Figure 4.8. Magnitude of the reflection coefficient of the designed slot fed by a rectangular waveguide.

over 530-MHz bandwidth. Consequently, using this slot, the overall system becomes more robust against signal source drifts.

In general, the simulation results are in good agreement with the measurement results. The small discrepancies such as the shift in resonance frequency may be attributed to the manufacturing tolerance margins in material and dimensions (which can not be accounted for in simulations), as well as change of diode parameters around their nominal values.

4.2.3. Transmission Measurements. Although the reflection experiments discussed above validates the basic slot design, i.e., resonance frequency, it is imperative to study the slot modulated response in a typical transmission-through setup (as it will be used in the imaging array). Figure 4.9 shows the measurement setup and results of a through transmission experiment. An antenna connected to port 1 of the HP8510C VNA was used illuminate the slot from 12.5 cm (5 in) away. The slot was mounted on the aperture a waveguide connected to port 2 of the VNA. The measured baseband complex signal, i.e., S_{21}, is shown in polar format in Figure 4.9(a). The

small transmission coefficient seen near zero when the slot is closed indicates very small signal gets transmitted through the slot. When the slot is open, maximum signal passes through the slot to the receiver of the VNA. The magnitude and phase of the complex signal **S**, the vector difference between the signals received when the slot is open and closed as depicted in Figure 4.9(a), corresponds to those of the incident signal. Just like modulated dipoles, ideal detection should consider the vector difference, **S**, between the received signals for both modulation states.

Figure 4.9(b) shows the baseband measured signal as the slot is modulated over time between the open and closed states in rectangular magnitude/phase format. The magnitude difference between signals received when the slot is open and closed is as high as 15 dB which indicates very strong modulation as it will be quantified next.

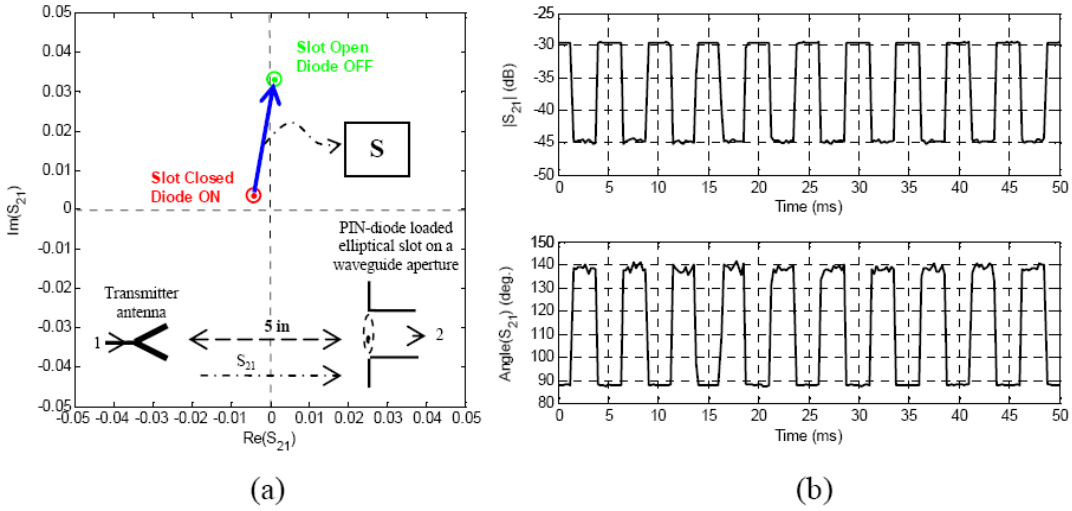

Figure 4.9. The baseband signal transmitted through the slot represented in (a) polar and (b) rectangular magnitude/phase formats.

4.2.4. Modulation Response. The modulation depth is the ultimate figure-of-merit which truly establishes the utility of the designed slot as a modulated element in an imaging array. The baseband signal measurements performed using the VNA as presented above can not be used to estimate the modulation depth accurately

(the VNA has a narrow-band tuned-receiver which cannot be used to measure the 24 GHz carrier signal and the modulation sidebands at the same time). To measure the modulation depth, the designed slot was modulated at 20 kHz and the spectrum of the received signal was measured using a spectrum analyzer. For ideal ON-OFF modulation, the modulated signal will be 6.02 dB below the carrier when the slot is completely opened and closed in modulation. As shown in Figure 4.10, with the designed slot, the fundamental signal harmonic is 6.33 dB below the carrier (dBc), i.e., 0.31 dB deviation from the ideal case. This small discrepancy arises from small signal leakage and losses when the slot closed and opened, respectively (as it can be noted from the above simulation and measurement results).

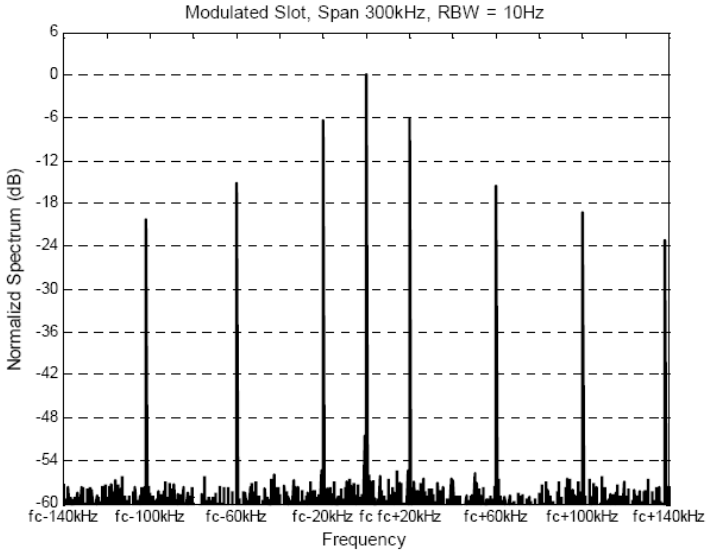

Figure 4.10. Measured normalized spectrum of the signal received through the K-band slot, $f_c = 24$ GHz.

The slot modulation depth is calculated from the spectrum measurements presented in Figure 4.10, i.e., using (67), to be 96.5%. Such a high modulation depth is attributed to the unique design of the slot where it can, almost completely, be opened and closed. At this point, it is interesting to compare the modulation

depth obtained using the designed slot with that of $\lambda/2$ (cf. Figure 3.3) and $\lambda/4$ (cf. Figure 3.4) dipole elements. Table 4.2 lists typical modulated signals level, relative to the carrier (D in dBc), as received from these loaded elements and the corresponding modulation depths in bistatic arrangements at 24 GHz. It is clear that the modulation depth using the designed slot is significantly higher compared to dipole elements case.

Table 4.2. Comparison between the measured modulation depths for four loaded elements.

Element	D (dBc)	**Modulation Depth (%)**
Elliptical Slot	6.33	96.5
$\lambda/2$-Dipole	41	1.8
$\lambda/4$-Dipole	50	0.63

As opposed to the conventional MST based on modulated dipole elements, detecting a modulated signal that is 6 dB below the carrier such as the one resulting from modulating the designed slot is not problematic. In this case, proper amplification can be used to boost the modulated signal level without saturating the receiver front-end as in the conventional MST systems. Besides improving the system sensitivity by the virtue of increasing the modulation depth, the residual carrier suppressing procedures routinely used with the conventional MST imaging arrays are not needed when the designed slot is utilized. This enhances the robustness of the imaging system.

4.2.5. Design Enhancement. The modulated response of the slot is affected by the signals leaking from/to biasing structure, i.e. the line used to control the PIN diode. In the design demonstrated above, small surface mount (SMT) decoupling capacitors were used to reduce this coupling (see Figure 4.7), and consequently, enhance the modulation depth. In 2D imaging arrays where hundreds of slots may be used, mounting such capacitors on each slot may be costly and time consuming. A simple remedy is to route the bias line on the bottom PCB conductor using vias. At high frequencies, a cross-layer via presents high-inductive impedance, and hence, it achieves the required signal decoupling without the need for SMT capacitors.

To illustrate the above idea, consider Figure 4.11(a) which shows schematics of the unloaded slot without biasing components, i.e., SMT capacitors, and two unloaded slot designs with different bias line routing. One of designs uses bias line components, i.e., SMT capacitors, just like the design considered earlier. The second loaded slot design does not incorporate any SMT capacitors and uses vias to route the bias line instead as shown Figure 4.11(a). The magnitude of the measured reflection coefficient for each of these three slots is shown in Figure 4.11(b).

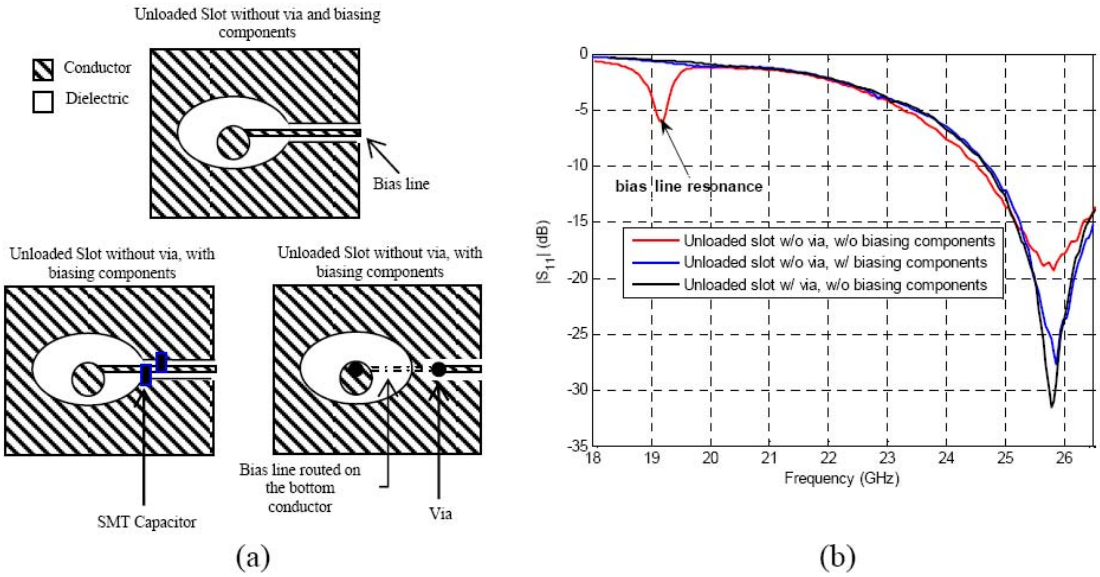

Figure 4.11. (a) Schematics of unloaded elliptical slots with different bias line routing, and (b) the measured magnitude of the reflection coefficient, S_{11}, corresponding to the slots shown in part (a).

When neither SMT capacitors nor vias are used, signals couple into the bias line and it shows up as relatively low-frequency resonance in the measured response (the resonance is due to higher-order slot mode. Generating this mode requires energy to be taken away from the dominant mode). In this case, the minimum measured response is around -19 dB. Using SMT capacitors reduces the coupling to the bias line (its resonance disappears) and causes the minimum reflection to become -27 dB

(getting better). The reflection response with vias, not only reduces the bias line coupling but also reduces the slot reflection further (-31 dB) compared to routing using SMT capacitors as shown in Figure 4.11(b). This in effect improves the slot performance (how well it opens and closes). Note that adding the SMT capacitors and vias change the resonance frequently slightly. This shift was accounted for in order to make the point about the minimum reflection in each case.

4.3. SUMMARY

A novel modulated slot design has been proposed and tested. The proposed slot is aimed to replace the inefficient small dipoles used in conventional MST-based imaging systems. The developed slot is very attractive as MST array element due to its small size and high efficiency/modulation depth. In fact, the developed slot has been successfully used to implement the first prototype of a microwave camera operating at 24 GHz. It is also being used in the design of the second generation of the camera [18].

Finally, the designed elliptical slot can be used as an electronically controlled waveguide iris for many other purposes (for instance in constructing waveguide reflective phase shifters and multiplexers/switches)